Earthquake Engineering, Tenth World Conference © 1992 Balkema, Rotterdam. ISBN 90 5410 060 5

Propagation characteristics of seismic motion in Ashigara Valley, Japan

S. Higashi
Central Research Institute of Electric Power Industry, Japan

K. Kudo
Earthquake Research Institute, University of Tokyo, Japan

ABSTRACT: We have made array analysis of long-period (1 - 15 s) strong motion in Ashigara Valley, Japan. From the frequency-wavenumber analysis combined with the polarization analysis, we found significant variation of the propagation direction of Love waves in the sedimentary basin. They did not coinside with the source azimuth for the event. One of the Love wave arrivals incident on the valley turned to its propagation path and amplified in the valley. Not only the underground structure beneath Izu Peninsula but the three-dimensional stucture of the valley may affect the propagation characteristics of seismic waves in the valley.

1 INTRODUCTION

An understanding of propagation characteristics of seismic motion in sedimentary basin is essential for estimating the damage distribution from an earthquake. It has been recognized that the long-period (1-15 s) strong motion is prominent in sedimentary basins and the contribution of surface waves is considerable for amplifying and prolonging the earthquake motion due to vertical strong heterogeneity. Swanger and Boore (1978) and Kudo (1978) have shown that the synthetics by a normal mode solution assuming a flat layering structure model simulated closely the observed displacements from an earthquake at a shallow depth. Vidale and Helmberger (1988) and Yamanaka et al. (1989) extended their discussions on surface wave propagation in laterally heterogeneous media by using a finite difference method.

In order to investigate propagation characteristics, it is necessary to identify wave types and propagation direction of seismic waves. Particle motion analysis is a simple but useful method for identifying the types of seismic waves. Vidale (1986) proposed a polarization filter which gives us the azimuth and dip of the direction of maximum polarization and the degree of elliptical polarization of the complex seismic motion as a function of time. However, when using this analysis alone, it is difficult to determine the wave type in cases where propagation path is not uniform. Array observation data would be helpful in overcoming this difficulty. The frequency-wavenumber spectral analysis is useful in determining the phase velocity and azimuth of seismic waves as a function of time.

In this paper, we will combine these two methods for discriminating the wave types and propagation characteristics of long-period strong motion using the array observation data obtained in Ashigara Valley, Japan.

2 SUMMARY OF ARRAY OBSERVATION

The Ashigara Valley, located about 80 km south-west of Tokyo, is an alluvial basin 12 km long and 4 km wide. Its longitudinal axis runs northwest-southeast. The basin is surrounded by low mountains: the Oiso hills on the east side, the Tanzawa mountains on the north side, and the Hakone Volcanos on the west side. Deposits found in the basin consist mostly of clay, sand and gravel by the sedimentation along the Sakawa River and other small rivers. Rock outcrops are found in the hill and mountain sides.

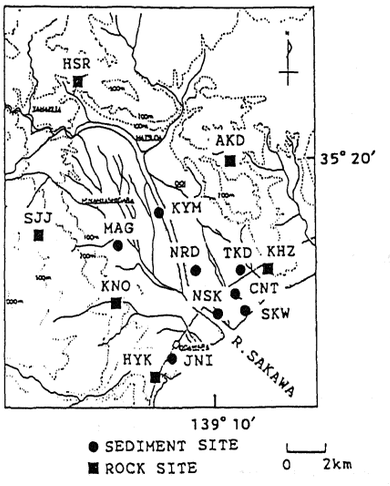

Figure 1. Location map of the digital strong motion accelerograph array in Ashigara Valley, Japan.

The digital strong-motion accelerograph array network was installed in the basin (Kudo et al. 1988). On the mountain sides, accelerographs are on outcrops of sedimentary or volcanic rock, while those in the basin are on the free surface of the soft sedimentary layers (Fig. 1).

The data used in this study are from the Izu-Oshima Kinkai earthquake of Feb. 20, 1990 (34°45.6′ N, 139° 14.0′ E, D=5.8 km, M_{JMA}=6.5). The epicenter of the event is located south looking from the Ashigara Valley (Fig. 2). The velocity seismograms were obtained by performing a numerical integration to the high-pass-filtered accelerations (pass frequency is 0.033 Hz). Then the three components of the velocity records were rotated into radial, transverse and vertical components.

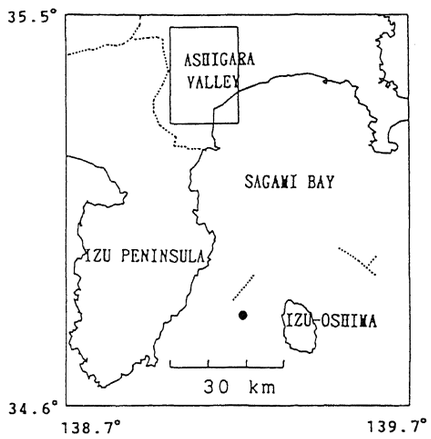

Figure 2. Location map of the Ashigara Valley and the epicenter of the Feb. 20, 1990 Izu-Oshima Kinkai earthquake.

3 METHODS

3.1 *Polarization analysis*

The complex polarization analysis proposed by Vidale(1986) was used in this analysis. This method can handle elliptical polarization by the use of the analytic signal. A three-component seismogram is rotated into the radial ($u_r(t)$), transverse ($v_r(t)$), and vertical ($w_r(t)$) components and is converted to an analytic three-component seismogram as follows.

$$\begin{aligned} u(t) &= u_r(t) + jH[u_r(t)] \\ v(t) &= v_r(t) + jH[v_r(t)] \\ w(t) &= w_r(t) + jH[w_r(t)] \end{aligned} \tag{1}$$

where H represents the Hilbert transform and j stands for $\sqrt{-1}$. The covariance matrix of the analytic signals is

$$C(t)=\begin{pmatrix} uu^* & uv^* & uw^* \\ vu^* & vv^* & vw^* \\ wu^* & wv^* & ww^* \end{pmatrix} \tag{2}$$

where the asterisks represent complex conjugation. The three eigenvalues of the covariance matrix, and the eigenvector associated with the largest eigenvalue is $X=(x_0,y_0,z_0)$. Since the components of the eigenvector have complex values, it is necessary to rotate the eigenvector in the complex plane so that the length of the real part is maximized.

The elliptical component of polarization is

$$P_E=\frac{|\mathrm{Im}(\mathbf{X})|}{|\mathrm{Re}(\mathbf{X})|}, \qquad 0\le P_E\le 1. \tag{3}$$

P_E equals 1 for circular polarization, while P_E equals 0 for linear polarization. The strike and dip of the direction of maximum polarization are written as follows;

$$\theta = \tan^{-1}\frac{\mathrm{Re}(z_0)}{\sqrt{\mathrm{Re}(x_0)^2+\mathrm{Re}(y_0)^2}}, \quad -90^\circ \le \theta \le 90^\circ, \tag{4}$$

$$\delta = \tan^{-1}\frac{\mathrm{Re}(y_0)}{\mathrm{Re}(x_0)}, \qquad -90^\circ \le \delta \le 90^\circ. \tag{5}$$

In order to improve the signal to noise ratio of S-wave and later phase arrivals, a measure of the strength of polarization defined by Vidale (1986) is modified into

$$P_S = \frac{\lambda_0}{\lambda_{max}}\left(1-\frac{\lambda_1+\lambda_2}{\lambda_0}\right), \qquad 0 \le P_S \le 1, \tag{6}$$

where is the maximum eigenvalue of the record. The arrival is assumed to be a signal when particle motion is polarized stronger than a certain level of P_S. However, a proper level of P_S depends on the record and it is left to one's discretion.

3.2 *Frequency-wavenumber spectral analysis*

The high resolution method proposed by Capon (1969) was used to determine the propagation directions and apparent velocities of waves identified by the polarization analysis. The estimate of the power spectrum is

$$P(\mathbf{k},\omega) = \left[\mathbf{U}^t(\mathbf{k})\mathbf{S}^{-1}(\omega)\mathbf{U}(\mathbf{k})\right]^{-1} \tag{7}$$

where $\mathbf{k}$ is the wavenumber vector and ω the frequency. $\mathbf{U}(\mathbf{k})$ is the beamsteering vector and $\mathbf{U}^t(\mathbf{k})$ is its complex conjugation. The elements of the vector are

$$U_i(\mathbf{k}) = \exp\{j\mathbf{k}\cdot\mathbf{x}_i\}$$

where x_i is the location of the i-th observation point. $\mathbf{S}(\omega)$ is the cross-spectral matrix. The cross-spectral estimates are normalized to unit amplitude in order to reduce site amplification effects.

4 RESULTS OF POLARIZATION AND FREQUENCY-WAVENUMBER ANALYSES

From the results of the running spectral analysis, we divided the seismograms into three wave groups. The first group is the 10 - 15 s period wave which appears on the transverse component just after the first S wave arrival (A in Fig. 3). The second group has a predominant period of 5 - 8 s (B1 in Fig. 3) and appears on both the radial and transverse components. The last one appears on the transverse component and has a period of around 10 s (B2 in Fig. 3).

The 10 - 15 s period arrival (A) consists of either a Love wave or SH wave which has a horizontal, linear polarization with a strike of +/-80°. The later arrivals are also horizontally and linearly polarized. However, the strike of the maximum polarization of the B1 group is -40°, while that of the B2 group is +/-90° (Fig. 3). The figures of the left side of Fig. 4 shows the horizontal components of eigenvectors of the A, B1 and B2 groups for the time windows indicated by thick lines in Fig.3, respectively. Frequency-wavenumber spectra of these arrivals for the corresponding time windows are given in the right side of Fig.4. The phase velocity for the A group is 2.7 km/s at the period of 11s, while 2.4 km/s at 9.1s for the B2 group. The directions of both groups are 10 - 15° west of the azimuth of the event. For the B1 group which is predominant in the radial component, the strikes of maximum polarization are -40° at the stations near the coast of the valley, while at the other stations they are diverted (Fig. 4). The group does not propagate from a source azimuth but from 50° west of the source azimuth, having a velocity of 2.1 km/s at 5.0 s (Fig. 4).

From the analyses for the data of the sediment sites in the valley, the B1 group is polarized perpendicular to the propagation direction. Therefore, the B1 arrival is indicated as Love wave. On the other hand, using all stations, the group arrives from 30° west of the source azimuth (Fig. 5). This indicates that the Love waves incident on the valley turned to more easterly path and were amplified in the sedimentary layers. The amplitudes of vertical components were approximately one-fifth of Love waves, therefore, examination on Rayleigh waves is deferred to an analysis of another event.

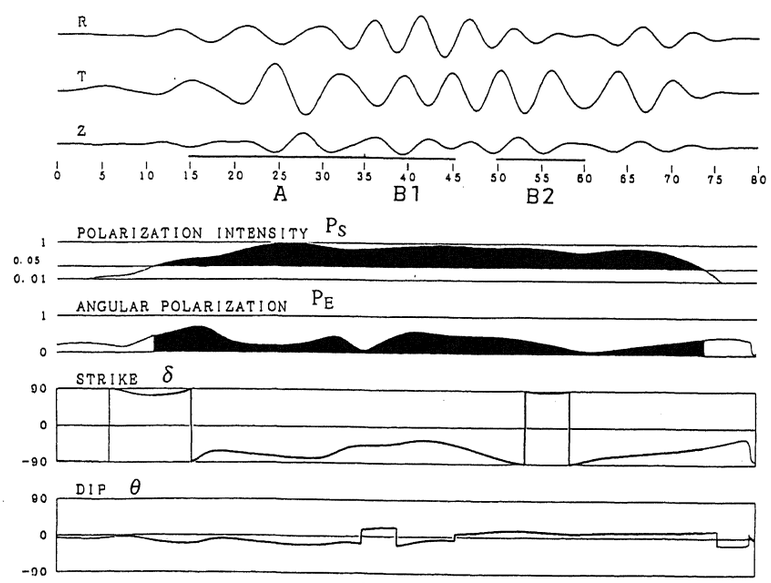

Figure 3. Polarization analysis of the band-pass-filtered (0.1-0.2 Hz) seismograms obtained at station CNT. Time windows for the polarization and frequency-wavenumber spectrum analyses are shown in the figure.

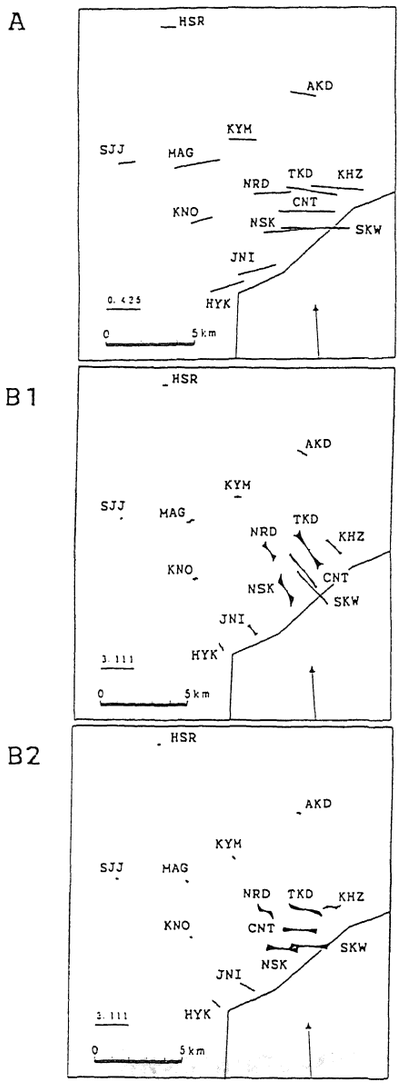

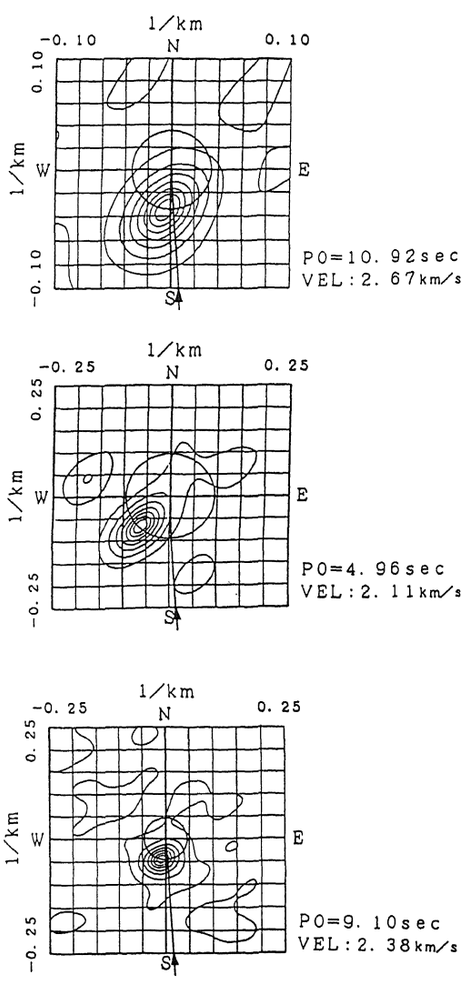

Figure 4. Left: Horizontal components of maximum polarization for the time windows, A, B1 and B2, indicated in Figure 3. The large arrow indicates the direction away from the source. Right: Frequency-wavenumber spectra for the same time windows.

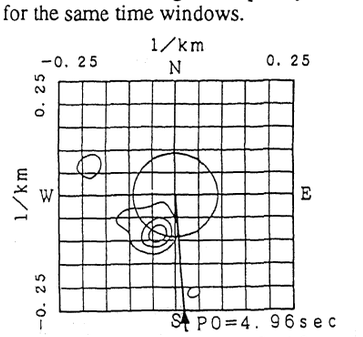

Figure 5. Frequency-wavenumber spectrum for B1 arrival using all stations.

5 LOVE WAVE DISPERSION

We found Love waves of this event has a clear dispersion from the results of the frequency-wavenumber spectral analysis. Figure 6 shows the phase velocities of Love waves for the event plotted against periods. Solid line in Fig. 6 shows the dispersion curve of the fundamental mode of Love waves calculated for the model of Fig. 7. The shallow structure model was estimated from the data of a down hole seismic prospecting at CNT. The intermidiate and deep structure model was determined by the seismic explosion experiments in the Ashigara Valley (Japanese Working Group on Effects of Surface Geology on Seismic Motion 1989) and structure model in the Izu Peninsula (Asano et al. 1982,1985; Yoshii et al. 1985,1986; Kudo et al. 1978). The phase velocities of Love waves match well with the dispersion curve of the fundamental mode in the sedimentary layers of the valley. This fact confirms the amplification of Love waves in the valley.

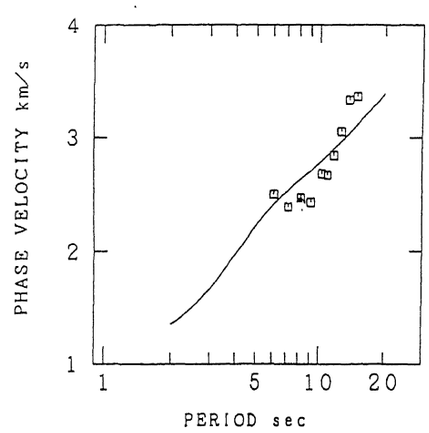

Figure 6. Dispersion curve of the fundamental mode of Love waves.

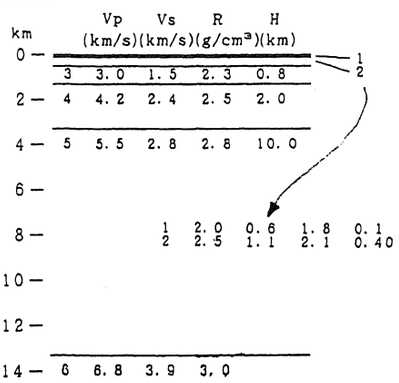

Figure 7. Flat layering model for calculating dispersion curve. Vp and Vs represent P-wave and S-wave velocities, respectively. R and H indicate density and thickness.

6 CONCLUSIONS

The effects of a sediment-filled valley on seismic wave propagation were investigated using the strong motion accelerograph array in the Ashigara Valley, Japan. From the frequency-wavenumber spectral analysis combined with the polarization analysis, we found significant variation in the propagation direction of Love waves. The Love waves incident on the valley turned to a more easterly propagation path and were amplified in the valley. The three dimensional heterogeneity probably caused the variation of propagation path. We also found that the propagation direction of seismic waves did not coincide with the source azimuth for the event. The underground structure beneath Izu Peninsula may affect the propagation path of the seismic waves.

REFERENCES

Asano, S., T. Yoshii, S. Kubota, Y. Sasaki, H. Okada, S. Suzuki, T. Masuda, H. Murakami, N. Nishide & H.Inatani 1982. Crustal structure in Izu Peninsula, Central Japan, as derived from explosion seismic observations. 1. Mishima-Shimoda profile. *J. Phys. Earth* 30: 367-387.

Asano, S., K. Wada, T. Yoshii, M. Hayakawa, Y. Misawa, T. Moriya, T. Kanazawa, H. Murakami, F. Suzuki, R. Kubota, and K. Suyehiro 1985. Crustal structure in the northern part of the Philippine Sea plate as derived from seismic observations of Hatoyama-Off Izu Peninsula explosions. *J. Phys. Earth* 33: 173-189.

Capon, J. 1969. High-resolution frequency-wave-number spectrum analysis. *Proc. IEEE*: 1408-1418.

Japanese Working Group on the Effects of Surface Geology on Seismic Motion, prepared by S.Higashi 1989. Underground structure beneath Ashigara Valley, Japan. *Proc. National Symposium on Effects of Surface Geology on Seismic Motion*: 199-206.

Kudo, K. 1978. The contribution of surface waves to strong ground motions, *Proc. 2nd Intern. Conf. Microzonation* 2: 765-776.

Kudo, K., S. Zama, M. Yanagisawa & E. Shima 1978. On the shear wave underground structure of Izu Peninsula. *Bull. Earthq. Res. Inst.* 53: 779-792 (in Japanese).

Kudo, K., E. Shima, & M. Sakaue 1988. Digital strong motion accelerograph array in Ashigara Valley — Seismological and engineering prospects of strong motion observation. *Proc. 9th WCEE*: 119-124.

Swanger, H.J. & D.M. Boore 1978. Simulation of strong-motion displacements using surface-wave model superposition. *Bull. Seismol. Soc. Am.* 68: 907-922,.

Vidale, J.E. 1986. Complex polarization analysis of particle motion. *Bull. Seismol. Soc. Am.* 76: 1393-1405.

Vidale, J.E. & D.V. Helmberger 1988. Elastic finite-difference modeling of the 1971 San Fernando, California earthquake. *Bull. Seismol. Soc. Am.* 78: 122-141.

Yamanaka, H., K. Seo & T. Samano 1989. Effects of sedimentary layers in surface-wave propagation. *Bull. Seismol. Soc. Am.* 79: 631-644.
Yoshii, T., S. Asano, S. Kubota, Y. Sasaki, H. Okada, T. Masuda, T. Moriya, & H. Murakami 1985. Crustal structure in Izu Peninsula, Central Japan, as derived from explosion seismic observations. 2. Ito-Matuzaki profile. *J. Phys. Earth* 33: 435-451.
Yoshii, T., S. Asano, S. Kubota, Y. Sasaki, H. Okada, T. Masuda, H. Murakami, S. Suzuki, T. Moriya, N. Nishide & H. Inatani 1986. Detailed crustal structure in the Izu Peninsula as revealed by explosion seismic experiments. *J. Phys. Earth* 34: S241-S248.